

ORIGINAL ARTICLE

Characterization of NaCl tolerance in *Desulfovibrio vulgaris* Hildenborough through experimental evolution

Aifen Zhou¹, Edward Baidoo², Zhili He¹, Aindrila Mukhopadhyay², Jason K Baumohl², Peter Benke², Marcin P Joachimiak², Ming Xie¹, Rong Song¹, Adam P Arkin², Terry C Hazen^{3,4}, Jay D Keasling², Judy D Wall⁵, David A Stahl⁶ and Jizhong Zhou^{1,7,8}

¹Institute for Environmental Genomics, Department of Microbiology and Plant Biology, University of Oklahoma, Norman, OK, USA; ²Physical Biosciences Division, Lawrence Berkeley National Laboratory, Berkeley, CA, USA; ³Department of Civil and Environmental Engineering, The University of Tennessee, Knoxville, TN, USA; ⁴Biosciences Division, Oak Ridge National Laboratory, Oak Ridge, TN, USA;

⁵Biochemistry and Molecular Microbiology and Immunology Departments, University of Missouri, Columbia, MO, USA; ⁶Department of Civil and Environmental Engineering, University of Washington, Seattle, WA, USA;

⁷Earth Sciences Division, Lawrence Berkeley National Laboratory, Berkeley, CA, USA and ⁸State Key Joint Laboratory of Environment Simulation and Pollution Control, School of Environment, Tsinghua University, Beijing, China

***Desulfovibrio vulgaris* Hildenborough strains with significantly increased tolerance to NaCl were obtained via experimental evolution. A NaCl-evolved strain, ES9-11, isolated from a population cultured for 1200 generations in medium amended with 100 mM NaCl, showed better tolerance to NaCl than a control strain, EC3-10, cultured for 1200 generations in parallel but without NaCl amendment in medium. To understand the NaCl adaptation mechanism in ES9-11, we analyzed the transcriptional, metabolite and phospholipid fatty acid (PLFA) profiles of strain ES9-11 with 0, 100- or 250 mM-added NaCl in medium compared with the ancestral strain and EC3-10 as controls. In all the culture conditions, increased expressions of genes involved in amino-acid synthesis and transport, energy production, cation efflux and decreased expression of flagellar assembly genes were detected in ES9-11. Consistently, increased abundances of organic solutes and decreased cell motility were observed in ES9-11. Glutamate appears to be the most important osmoprotectant in *D. vulgaris* under NaCl stress, whereas, other organic solutes such as glutamine, glycine and glycine betaine might contribute to NaCl tolerance under low NaCl concentration only. Unsaturation indices of PLFA significantly increased in ES9-11. Branched unsaturated PLFAs i17:1 ω9c, a17:1 ω9c and branched saturated i15:0 might have important roles in maintaining proper membrane fluidity under NaCl stress. Taken together, these data suggest that the accumulation of osmolytes, increased membrane fluidity, decreased cell motility and possibly an increased exclusion of Na⁺ contribute to increased NaCl tolerance in NaCl-evolved *D. vulgaris*.**

The ISME Journal (2013) 7, 1790–1802; doi:10.1038/ismej.2013.60; published online 11 April 2013

Subject Category: Integrated genomics and post-genomics approaches in microbial ecology

Keywords: *D. vulgaris*; experimental evolution; salt adaptation; transcriptomics; metabolites assay; PLFA analysis

Introduction

Desulfovibrio vulgaris is a member of the dissimilatory sulfate-reducing bacteria (SRB) widely distributed in anaerobic environments, such as gas

pipelines, subsurface tanks, sediments and off-shore petroleum production facilities (Postgate, 1984). Much research has focused on *D. vulgaris* as a model to explore the SRB that have important roles in the biogeochemical cycling of sulfur, carbon and nitrogen and potentially the bioremediation of toxic heavy metals and radionuclides. In addition, SRB have been identified as culprits in the biocorrosion of ferrous metal installations in the petroleum industry and concrete structures in wastewater collection systems (Muyzer and Stams, 2008; Zhou *et al.*, 2011). Effective reduction of highly toxic

Correspondence: J Zhou, Institute for Environmental Genomics (IEG), Department of Microbiology and Plant Biology, University of Oklahoma, Norman, OK 73019, USA.

E-mail: jzhou@ou.edu

Received 25 August 2012; revised 1 March 2013; accepted 9 March 2013; published online 11 April 2013

Cr (VI) or U (VI) to less toxic Cr (III) or U (IV) by *D. vulgaris* Hildenborough has been reported (Lovley *et al.*, 1993; Lovley and Phillips, 1994; Elias *et al.*, 2004), and *D. vulgaris* was found to exist in uranium (VI) contaminated field site (Chang *et al.*, 2001). High NaCl concentration is also present in several DOE (Department of Energy) sites contaminated with toxic metals. Therefore, evolving NaCl-tolerant *D. vulgaris* strains and identifying the NaCl adaptation mechanisms could have important consequences for bioremediation strategies and the prediction of biocorrosion for the petroleum industry.

Several aspects of the NaCl stress responses in microorganisms have been studied. Intracellular accumulation of cocktails of organic solutes has been shown to be one of the major strategies to cope with osmotic stress caused by high concentrations of NaCl (Roberts, 2005). In the model Gram-negative bacterium, *Escherichia coli*, glutamate (Glu), proline, glycine betaine (GB), ectoine and trehalose accumulated during osmotic stress (Jebbar *et al.*, 1992; Strøm and Kaasen, 1993; McLaggan *et al.*, 1994). Glu was found to be the primary osmolyte in other microorganisms, such as *Salmonella typhimurium* (Botsford *et al.*, 1994) and *Rhizobium meliloti* (Botsford and Lewis, 1990). GB and proline have been reported to be important osmolytes in *Listeria monocytogenes* (Ko *et al.*, 1994) and *Bacillus subtilis* (Whatmore *et al.*, 1990), respectively. GB and trehalose were the major compatible solutes in the moderately halophilic SRB *Desulfovibrio halophilus* (Welsh *et al.*, 1996). In *D. vulgaris*, GB and ectoine were found to be important for relieving NaCl stress caused by exposure to 250 mM NaCl for 4 h (Mukhopadhyay *et al.*, 2006). By contrast, accumulation of Glu (eightfold) and alanine (Ala, 1.8-fold) was detected in *D. vulgaris* exposed to 250-mM NaCl stress for about 100 h (He *et al.*, 2010). However, the osmoprotectants that counteract the osmotic stress caused by NaCl during evolutionary adaptation of *D. vulgaris* are unknown. Other NaCl tolerance mechanisms include changes of membrane lipid composition to compensate for the decrease in membrane fluidity. Levels of unsaturated fatty acids in membrane lipids increased in *B. subtilis* under osmotic stress (López *et al.*, 2000; Los and Murata, 2004). An increase of branched fatty acids in Gram-positive halophilic and halotolerant bacteria or unsaturated fatty acids in Gram-negative and Gram-positive halophilic bacteria increases the membrane fluidity when grown in media with increasing salt concentrations (Kates, 1986; Russell, 1989). In *D. vulgaris*, an increase of unsaturated branched fatty acid i17:ω9c was detected in response of *D. vulgaris* to NaCl shock (Mukhopadhyay *et al.*, 2006). Any changes in phospholipid fatty acid (PLFA) composition during evolutionary NaCl adaptation of *D. vulgaris* remain to be determined.

Salt-stress tolerance is a polygenic trait especially attractive for evolutionary studies (Dhar *et al.*, 2011).

Considering the complexity of interactions between natural environments and microorganisms, it is challenging to understand how microorganisms respond to stresses and then adapt genetically. The response of *D. vulgaris* to NaCl shock (Mukhopadhyay *et al.*, 2006) and 100-h exposure (He *et al.*, 2010) have been reported. In addition, experimental evolution of microorganisms under controlled laboratory conditions have been established (Elena and Lenski, 2003). Therefore, we aimed to reveal the possible adaptation mechanism of *D. vulgaris* developed through experimental evolution under NaCl stress by transcriptomic, metabolite and PLFA analyses.

Towards this goal, NaCl-adapted strains of *D. vulgaris* was obtained after culturing for 1200 generations in medium amended with 100 mM NaCl. Examination of single-colony isolates from the NaCl-evolved cultures indicated that the accumulation of organic osmolytes, increased membrane fluidity, increased exclusion of Na⁺ and decreased cell motility contribute to the increased NaCl tolerance.

Materials and methods

Bacterial strains and growth conditions

A clonal isolate of *D. vulgaris* Hildenborough (ATCC 29579) was used as the ancestor (An) to found 12 populations for experimental evolution. Six populations (EC, population Nos. 1–6) were subsequently propagated in control environment (defined medium LS4D with 60 mM lactate as electron donor and 50 mM sulfate as electron acceptor, no supplemented NaCl, total [Na⁺] is about 210 mM; Mukhopadhyay *et al.*, 2006) and six populations (ES, population Nos. 7–12) propagated in a constant NaCl stress environment (LS4D with additional 100 mM NaCl, total [Na⁺] is about 310 mM) for 1200 generations. The cell cultures were grown at 37 °C anaerobically and serially transferred every 48 h with a 1–100 dilution. Single-colony isolates (strains designated as EC3-10 and ES9-11) from the evolved populations EC No.3 or ES No.9, respectively, were obtained by plating and single-colony isolation.

Analysis of growth data

Growth phenotypes of the ancestral strain (An) and evolved strains ES9-11 and EC3-10 in control medium LS4D or NaCl stress medium (LS4D + 250 mM NaCl) were examined with three replicates for each strain. Growth rate and yield were obtained independently from the growth curve of each replicate. Yield was the maximum OD₆₀₀ (optical density measured at the wavelength of 600 nm) reached by the culture and the growth rate was 2.303 × the slope of the linear portion of the growth curve obtained by plotting log₁₀(OD₆₀₀) with time.

Biomass production

Freezer stocks of the ancestral strain An and the evolved strains, ES9-11 and EC3-10, were inoculated into 10 ml LS4D with 1–100 dilution and grown to stationary phase. These cultures (1 ml) were then inoculated into the production vessels containing 100 ml of LS4D supplemented with different concentrations of NaCl (0, 100 or 250 mM). All samples were prepared in triplicates. The mid-exponential phase cultures ($OD_{600} \sim 0.4$ with exception of $OD_{600} \sim 0.25$ for the An strain grown in LS4D + 250 mM NaCl) were harvested by centrifugation at 6000 g for 10 min at 4 °C with 50 ml cell culture in each Falcon tube and the biomass was frozen in liquid nitrogen and kept at –80 °C for transcript and metabolite assays.

Isolation of total RNA, genomic DNA and fluorescence labeling

Isolation, purification and fluorescence labeling of total cellular RNA were performed as described previously (Chhabra *et al.*, 2006). Genomic DNA was isolated from *D. vulgaris* with CTAB method (Zhou *et al.*, 1996). Total RNA and genomic DNA were labeled with fluorescent dye Cy5 or Cy3, respectively. Cy5-labeled cDNA and Cy3-labeled gDNA were dried and stored at –20 °C before hybridization.

Microarray hybridization and data analysis

The *D. vulgaris* whole-genome oligonucleotide (70mer) microarray covering 3482 of the 3531 protein-coding sequences of the *D. vulgaris* genome (He *et al.*, 2006) was used for transcriptomics analysis. Array hybridizations were carried out with TECAN hybridization station (TECAN HS4800, TECAN Group Ltd, Durham, NC, USA). Array hybridization and data analysis were performed as described previously (Mukhopadhyay *et al.*, 2006; Zhou *et al.*, 2010). Microarray data have been deposited in the NCBI GEO database under accession number GSE39675.

The similarities of transcriptional profiling among different samples were analyzed with detrended correspondence analysis and AnoSim. The transcript level of each open reading frame was calculated as the ratio of signal intensity of Cy5 to Cy3, and the genes detected in at least two out of three replicates were kept for statistical analysis.

Extraction and analysis of metabolites by LC-MS (liquid chromatography-mass spectrometry) or CE-MS (capillary electrophoresis-mass spectrometry)

Metabolites were extracted via a methanol/water/chloroform extraction procedure and analyzed with CE-MS and LC-MS (Baidoo *et al.*, 2008; He *et al.*, 2010). All solvents were of HPLC (high-performance liquid chromatography) or greater grade (Honeywell

Burdick and Jackson, Muskegon, MI, USA). Formic acid (>98% v/v) was purchased from Riedel-de Haën (Seelze, Germany). Chemical standards for amino acids were purchased from Sigma-Aldrich (St Louis, MO, USA). The stock solutions (200 μ M) for amino acids were prepared with methanol/water (50:50, v/v). The lyophilized extracts from freeze-dried biomass (pellet from 50 ml of cell culture with $OD_{600} \sim 0.4$ as described above) were reconstituted in 500 μ l of methanol–water (50:50, v/v) solution or diluted to ensure that metabolite concentrations were within the ranges of the calibration curves.

Cell motility assay

Mid-exponential phase cells (5 μ l, $OD_{600} \sim 0.4$) of the ancestral strain An and the evolved strains, ES9-11 and EC3-10 (precultured from glycerol stocks and grown for one growth cycle with LS4D as described above), were applied on the surface of soft agar (0.4% (w/v)) plates (LS4D or LS4D + 250 mM NaCl). The plates were cultivated at 37 °C anaerobically for 4 days and the colony diameters were measured.

PLFA assays

Pellets from 50 ml of late-exponential phase cultures were collected and frozen in liquid nitrogen. The PLFA assay was conducted by Microbial ID Inc. (Newark, DE, USA). Briefly, fatty acids were extracted and methylated and then analyzed on a gas chromatograph equipped with a flame ionization detector. Peaks were named by comparing the calibration mixture with Sherlock software (Microbial ID Inc.). Unsaturation index (UI) of PLFAs was calculated as $UI = ((C:1 \times 1) + (C:2 \times 2) + (C:3 \times 3) + (C:4 \times 4)) / 100$, where C:1, C:2, C:3 and C:4 represent fatty acid's proportion (%) with 1, 2, 3 and 4 double bonds, respectively) (Ruess *et al.*, 2007).

Results

Increased NaCl tolerance in evolved *D. vulgaris*

An additional 100 mM NaCl in growth medium LS4D (containing ca. 210 mM Na^+) slightly decreased the final biomass yield and extended the lag phase of *D. vulgaris*. By contrast, a significant decrease of final biomass yield (about 50%) and growth rate were observed when grown in LS4D amended with 250 mM NaCl (He *et al.*, 2010). We interpreted these observations to define the 100-mM NaCl amendment to be a low stress and 250-mM NaCl, a high stress condition. Therefore, LS4D + 100 mM NaCl was used as the stress condition for experimental evolution and LS4D + 250 mM NaCl was used for evaluation of NaCl tolerance in evolved *D. vulgaris*.

Significant improvement of tolerance to NaCl was observed in evolved *D. vulgaris* populations that had been cultured in unamended medium before challenging with 250 mM NaCl (Supplementary

Figure S1). In order to identify the adaptation mechanisms underlying the improved tolerance phenotype, single-colony isolates ES9-11 from population ES No.9 evolved in LS4D + 100 mM NaCl and EC3-10 from population EC No.3 evolved in LS4D were further investigated. The strains were each chosen as isolates with the best growth performance in LS4D + 250 mM NaCl from 15 randomly picked colonies from their respective populations. As shown in Figure 1 and Supplementary Figure S2, in LS4D + 250 mM NaCl, significant increases ($P < 0.0001$) of growth rate and final biomass yield, but shortened lag phase, were observed for evolved strains compared with the

ancestral strain, An, which had been maintained as a freezer stock. The growth rate of NaCl-evolved ES9-11 increased about fourfold (Figure 1a), and the final biomass yield was about twofold than that of ancestral An (Figure 1b), which were also significantly higher than that of control-evolved EC3-10 (growth rate, $P < 0.0001$; final biomass, $P = 0.0022$; Figures 1a and b). The lag phase (20.3 ± 0.6 h) in ES9-11 was significantly shorter than in EC3-10 (29.0 ± 1.0 h, $P = 0.0002$) and in An (107.8 ± 14.9 h, $P = 0.0005$) (Figure 1c). Similarly, in LS4D, better growth of ES9-11 was observed with significantly increased growth rate, final biomass and shortened lag phase compared with An (P -values 0.0213, 0.0022 and < 0.0001 , respectively) or EC3-10 (P -values 0.0065, 0.0034 and 0.0009 respectively). By contrast, the growth of EC3-10 was similar to An except for a significantly ($P < 0.0001$) shortened lag phase (Figure 1). These data demonstrated that strain ES9-11 evolved under NaCl stress appeared to be more tolerant to a challenge of higher NaCl than strain EC3-10 that was evolved in medium without NaCl amendment.

Transcriptional profiling changes in evolved *D. vulgaris*

The significant improvement of NaCl tolerance in NaCl-evolved ES9-11 encouraged us to explore the gene transcription changes. We hypothesized that genetic changes accumulated during evolution will be reflected in gene transcription profiling. The overall similarity of the transcription profiling among ancestral strain, NaCl-evolved ES9-11 and control-evolved EC3-10 is presented using a detrended correspondence analysis plot (Figure 2a). The three strains are separated by Axis 1, which explained 38.77% of the total variance. Low NaCl stress did not stimulate substantial changes in any of the strains, but the additional 250 mM NaCl in the medium induced the largest changes in the transcriptional profile of the ancestral strain, intermediate changes in the control-evolved EC3-10 and minimal changes in the NaCl-evolved ES9-11. Statistical tests with Anosim demonstrated the significant differences among the three strains: An vs ES9-11 ($R = 0.876$, $P = 0.001$), An vs EC3-10 ($R = 0.592$, $P = 0.001$), and two evolved strains ES9-11 and EC3-10 ($R = 0.807$, $P = 0.001$).

The number of genes with significant changes (cutoff values for $\log_2 R_{(\text{treatment/control})}$ and Z score were 1.5) also demonstrated significant differences among the three strains. As shown in Figure 2b, for strain An, 100-mM NaCl stress had almost no effect on transcription, whereas 250-mM NaCl stress had a major impact. A similar result, but dampened, was seen for the NaCl-evolved ES9-11, while a similar result but exaggerated was seen for the control-evolved EC3-10. Consistent with the minimal changes induced by 250-mM NaCl stress (Figure 2a), the smallest number of differentially

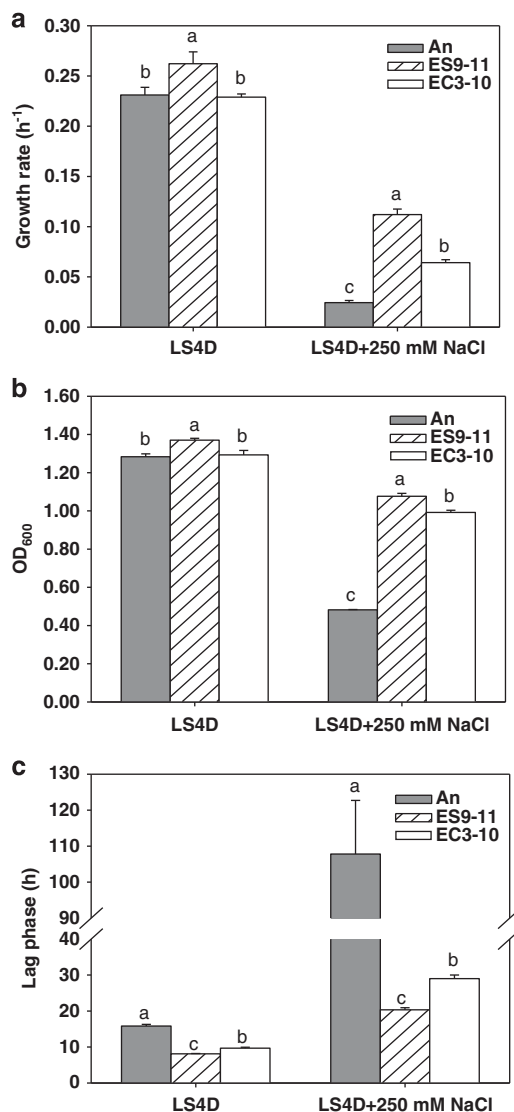


Figure 1 Improvement of NaCl tolerance in evolved *D. vulgaris* strains. The growth rates (a), biomass yields (b) and lag phases (c) of NaCl-evolved ES9-11, control-evolved EC3-10 and ancestral strain An in standard defined medium (LS4D) and high NaCl stress (LS4D + 250 mM NaCl) are shown. Averages of three biological replicates are shown. Error bars indicate s.d. The significance of differences among three strains is shown at the $P < 0.05$ level (t -test).

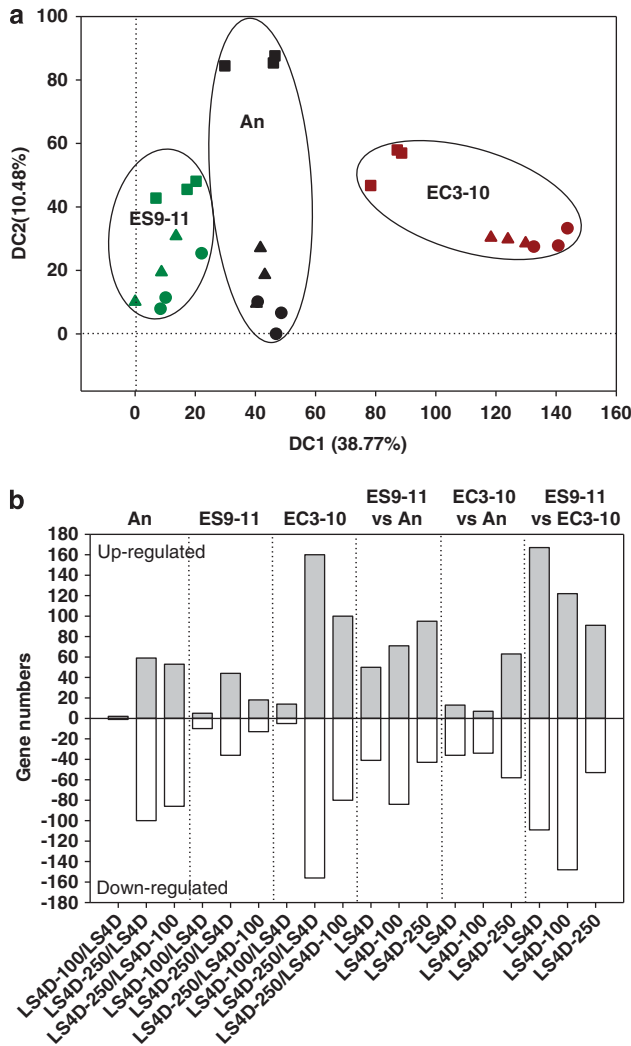


Figure 2 Distinct gene transcriptional profiling of evolved *D. vulgaris* strains. (a) The gene transcriptional profiling of NaCl-evolved ES9-11, control-evolved EC3-10 and ancestral strain An in medium with or without NaCl amendment are separated on detrended correspondence analysis plot. Each symbol represents a replicate sample. Circle, LS4D; triangle, LS4D + 100 mM NaCl; square, LS4D + 250 mM NaCl. (b) Numbers of differentially expressed genes (with cutoff values for $\log_2 R_{\text{treatment/control}}$ and Z score as 1.5) in medium with or without NaCl amendment. LS4D-100, LS4D + 100 mM NaCl; LS4D-250, LS4D + 250 mM NaCl.

expressed genes was detected in ES9-11 under 250-mM NaCl stress. Compared with An, in all the culture conditions, there were more differentially expressed genes in ES9-11 than in EC3-10. In addition, greater numbers of differentially expressed genes were found in ES9-11 compared with EC3-10 in all the culture conditions (Figure 2b). The results indicated that there were more gene expression changes in NaCl-evolved ES9-11 than in control-evolved EC3-10 under no-NaCl stress or NaCl stress conditions. Most of the differentially expressed genes in ES9-11 belonged

to the functional categories of amino-acid metabolism and transport, inorganic ion transport, cell motility, energy production and conversion, signal transduction mechanisms and transcription as described below (Tables 1–3).

Amino-acid synthesis and transport. Under no-NaCl stress, 100-mM NaCl or 250-mM NaCl stress conditions, ES9-11 had a significant increase in expression of DVU0593 encoding L-lysine exporter and DVU2615 encoding a family 3 bacterial extracellular solute-binding protein (Table 1). Under 250-mM NaCl stress, ES 9-11 had increased expression of genes DVU2341-DVU2343 in a three-gene operon encoding His/Glu/Gln/Arg/opine family amino-acid ABC transporter, of genes DVU2743 and DVU2744 in a five-gene operon encoding high-affinity branched-chain amino-acid ABC transporter, of DVU1378 encoding ketol-acid reductoisomerase (*ilvC*) involved in the biosynthesis of isoleucine or valine and of DVU3291 encoding the iron-sulfur cluster-binding subunit of Glu synthase. In addition, under NaCl stress conditions, ES-9-11 had a significant decrease in the expression of DVU1827 encoding acetylornithine deacetylase/succinyl-diaminopimelate desuccinylase family protein involved in the biosynthesis of lysine (Table 1).

Inorganic ion transport and metabolism. Under no-NaCl stress or 100-mM NaCl stress, ES9-11 had significant increases in the expression of genes DVU2571-DVU2574 involved in iron transport, but lack of further increase of expression under 250-mM NaCl stress (Table 1). Under 250-mM NaCl stress, strain ES9-11 had a significant increase in expression of DVU1778 encoding cation efflux family protein.

Cell motility. In all the conditions tested, ES9-11 had significant increases in expression of chemotaxis genes such as methyl-accepting chemotaxis protein (MCP) genes DVU3155 (*dcrH*) and DVU0170 and a general decrease in expression of 22 flagellar system related genes (Table 2). Under 250-mM NaCl stress, ES9-11 had significant increases in expression of DVU3182 (*dcrA*) and DVU1904 (*cheW-2*) compared with An (Table 2).

Energy production and conversion. Again under all the tested conditions, ES9-11 had significant increases in expression of genes involved in electron transfer system such as DVU0531-DVU0536 (*hmc* operon) and a cytochrome c gene DVU3107 compared with An (Table 3). Significant increases in the expression of a few other cytochrome genes under 250-mM NaCl stress were also seen in ES9-11. Under no-NaCl stress, ES9-11 had a significant increase in expression of DVU2645 encoding Na^+/H^+ antiporter family protein. Under no-NaCl stress and 100-mM NaCl stress, strain ES9-11 had a generally decreased expression of hydrogenase genes in the *coo* operon

Table 1 Expression changes of genes involved in amino-acid synthesis and transport or inorganic ion transport and metabolism in strain ES

DVU Nos.	Annotation	LS4D		LS4D-100		LS4D-250	
		ES vs An	ES vs EC	ES vs An	ES vs EC	ES vs An	ES vs EC
Amino-acid synthesis and transport							
DVU0593	L-lysine exporter, putative	2.75 (4.13)	2.39 (3.96)	2.36 (4.36)	1.48 (2.87)	4.29 (2.60)	2.51 (3.54)
DVU2615	Bacterial extracellular solute-binding protein, family 3	2.45 (4.20)	3.28 (4.70)	2.34 (4.34)	3.78 (5.72)	3.51 (2.43)	4.16 (4.59)
DVU1378	Ketol-acid reductoisomerase (<i>ilvC</i>)	0.05 (0.08)	0.18 (0.28)	0.45 (0.73)	0.41 (0.66)	1.10 (2.07)	1.26 (2.36)
DVU3291	Glutamate synthase, iron-sulfur cluster-binding subunit, putative	0.94 (0.99)	−0.49 (−0.59)	0.99 (0.81)	−0.30 (−0.27)	1.43 (1.42)	0.77 (0.71)
DVU2341	Amino-acid ABC transproter, permease protein, His/Glu/Gln/Arg/opine family	0.99 (1.89)	−0.08 (−0.15)	1.12 (2.13)	0.01 (0.02)	3.12 (1.89)	1.53 (2.77)
DVU2342	Amino-acid ABC transporter, periplasmic amino-acid-binding protein	0.57 (0.97)	0.18 (0.3)	0.96 (1.86)	0.09 (0.18)	2.19 (3.40)	1.50 (2.64)
DVU2343	Amino-acid ABC transporter, ATP-binding protein, <i>glnQ</i>	−0.24 (−0.35)	NA(NA)	1.23 (1.98)	0.77 (1.36)	1.07 (1.98)	NA
DVU2740 (<i>livF</i>)	High-affinity branched-chain amino-acid ABC transporter, ATP-binding protein	NA	NA	0.15 (0.16)	0.17 (0.16)	0.69 (1.06)	0.20 (0.18)
DVU2741 (<i>livG</i>)	High-affinity branched-chain amino-acid ABC transporter, ATP-binding protein	−0.14 (−0.21)	0.04 (0.05)	1.04 (1.06)	0.36 (0.38)	0.51 (0.72)	0.20 (0.29)
DVU2742 (<i>livM</i>)	High-affinity branched-chain amino-acid ABC transporter, permease protein	0.25 (0.31)	1.05 (1.56)	0.46 (0.71)	0.79 (1.22)	0.93 (0.96)	0.33 (0.42)
DVU2743 (<i>livH</i>)	High-affinity branched-chain amino-acid ABC transporter, permease protein	−0.35 (−0.3)	−1.24 (−1.33)	−0.80 (−1.36)	−1.83 (−2.55)	1.47 (0.93)	1.55 (1.06)
DVU2744	High-affinity branched-chain amino-acid ABC transporter, perisplasmic amino-acid-binding protein	0.48 (0.83)	0.10 (0.16)	0.14 (0.24)	−0.12 (−0.20)	2.26 (2.16)	0.89 (1.41)
DVU1827	Acetylornithine deacetylase/succinyl-diaminopimelate desuccinylase family protein	−0.48 (−0.79)	−0.76 (−1.28)	−1.05 (−1.48)	−1.35 (−1.87)	−1.14 (−1.82)	−0.45 (−0.65)
DVU0115	Shikimate 5-dehydrogenase (<i>aroE</i>)	−0.28 (−0.25)	−0.04 (−0.04)	0.20 (0.17)	0.25 (0.20)	−1.45 (−1.55)	−1.16 (−0.85)
DVU2492	N-(5-phosphoribosyl)anthranilate isomerase (<i>trpF-2</i>)	−0.08 (−0.10)	0.20 (0.25)	−0.31 (−0.29)	−0.52 (−0.52)	−1.52 (−1.52)	−1.27 (−1.46)
DVU3223	Aspartate aminotransferase (<i>aspB</i>)	−0.51 (−0.82)	−1.08 (−1.82)	−0.38 (−0.47)	−0.71 (−0.88)	−1.40 (−1.59)	−0.46 (−0.42)
Inorganic ion transport and metabolism							
DVU2571	Ferrous iron transport protein B (<i>feoB</i>)	2.26 (4.11)	2.28 (4.14)	2.69 (4.82)	2.73 (4.77)	−0.25 (−0.31)	2.98 (4.11)
DVU2572	Ferrous iron transport protein A, putative	1.45 (2.56)	2.26 (3.99)	1.87 (3.08)	2.30 (3.69)	−0.58 (−0.71)	2.61 (2.99)
DVU2573	Hypothetical protein	1.39 (2.59)	2.42 (4.59)	1.52 (2.56)	2.18 (3.75)	0.05 (0.09)	1.85 (2.95)
DVU2574	Ferrous ion transport protein, putative	1.16 (2.16)	2.65 (4.58)	1.17 (2.03)	2.00 (3.54)	0.37 (0.54)	1.42 (2.63)
DVU1778	Cation efflux family protein	0.80 (1.50)	0.96 (1.75)	0.91 (1.71)	1.04 (1.97)	2.18 (2.45)	0.91 (1.67)
DVU2477	Phosphate ABC transporter, periplasmic phosphate-binding protein, putative	−1.81 (−2.37)	−2.20 (−2.83)	−0.56 (−0.39)	0.20 (0.14)	−0.89 (−0.61)	−0.32 (−0.36)
DVU2478	Phosphate ABC transporter, permease protein, putative	−1.05 (−0.95)	−0.73 (−0.57)	−2.21 (−3.15)	−0.85 (−0.96)	−0.08 (−0.06)	−0.16 (−0.17)
DVU2479	Phosphate ABC transporter, permease protein, putative	−0.38 (−0.50)	−0.74 (−1.06)	0.25 (0.23)	−0.22 (−0.19)	−0.76 (−1.04)	−0.45 (−0.65)

Abbreviations: An, ancestor DvH; ATP, adenosine triphosphate; DVU, *Desulfovibrio vulgaris*; EC, strain isolated from population No.3 evolved under control condition; ES, strain isolated from population No.9 evolved under salt-stress condition; LS4D-100, LS4D + 100 mM NaCl; LS4D-250, LS4D + 250 mM NaCl; NA, not applicable.

Log₂R ratios are shown with Z score in parentheses. Boldface indicates more than twofolds of expression changes.

(DVU2286-2293). In addition, ES9-11 tended to increase the expression of two L-lactate permease family protein genes DVU2451 and DVU2683 under NaCl stress compared with An (Table 3).

Signal transduction and transcription. When compared with An, ES9-11 had significant increases in expression of genes DVU0598 and DVU0599

encoding putative carbon-starvation proteins in all the conditions (Table 3). Under no-NaCl stress or 10-mM NaCl stress conditions, ES9-11 had a significant increase in expression of DVU1967 encoding a transcriptional regulator. Under 250-mM NaCl stress, ES9-11 had significant increases in expression of genes DVU2114 (*atoC*, a sigma-54-dependent transcriptional regulator/response

Table 2 Expression changes of selected genes involved in cell motility in strain ES

DVU Nos.	Annotation	LS4D		LS4D-100		LS4D-250	
		ES vs An	ES vs EC	ES vs An	ES vs EC	ES vs An	ES vs EC
DVU0170	Methyl-accepting chemotaxis protein	2.20 (4.27)	3.38 (4.58)	1.51 (2.83)	2.85 (4.00)	2.54 (2.53)	2.74 (3.34)
DVU3155 (<i>dcrH</i>)	Methyl-accepting chemotaxis protein DcrH	1.87 (3.62)	2.09 (2.96)	1.79 (3.31)	2.66 (4.21)	2.64 (2.03)	3.80 (5.67)
DVU3182 (<i>dcrA</i>)	Methyl-accepting chemotaxis protein DcrA	1.00 (1.61)	0.73 (1.23)	0.95 (1.59)	0.78 (1.31)	2.10 (1.61)	1.77 (1.56)
DVU1904 (<i>cheW-2</i>)	Chemotaxis protein CheW	0.86 (1.61)	1.63 (2.85)	0.59 (1.10)	1.43 (2.48)	1.66 (3.03)	0.99 (1.83)
DVU1263	Type IV prepilin-like proteins leader peptidase (<i>pppA</i>)	1.28 (2.30)	1.46 (2.80)	1.13 (2.14)	1.35 (2.48)	2.54 (1.55)	2.45 (2.10)
DVU0307	Flagella basal body rod domain protein	-2.20 (-2.22)	-2.57 (-2.60)	-2.03 (-2.36)	-2.58 (-3.06)	-2.48 (-3.54)	-3.44 (-4.94)
DVU2444	Flagellin	-4.54 (-7.12)	-4.91 (-7.55)	-4.50 (-5.34)	-4.99 (-5.84)	-3.85 (-6.07)	-5.00 (-8.11)
DVU2445	Hypothetical protein	-4.20 (-6.79)	-4.59 (-7.23)	-3.69 (-4.94)	-4.47 (-5.66)	-3.54 (-3.64)	-4.79 (-4.94)
DVU2948	Bacterial flagellin N-terminal domain protein	-1.92 (-2.04)	-2.82 (-3.24)	-2.02 (-2.68)	-2.60 (-3.44)	-2.01 (-1.38)	-3.11 (-4.60)
DVU1441	Flagellin	-2.13 (-2.19)	-2.30 (-2.37)	-1.86 (-2.00)	-2.19 (-2.36)	-3.16 (-4.80)	-3.26 (-4.83)
DVU1442	Flagellin FlaG, putative	-0.59 (-1.14)	-0.93 (-1.64)	-1.04 (-1.04)	-1.47 (-1.53)	-1.56 (-1.02)	-1.76 (-1.18)
DVU1443 (<i>flgE</i>)	Flagellar hook protein FlgE	-1.68 (-1.55)	-2.29 (-2.14)	-2.70 (-1.90)	-3.14 (-2.23)	-3.63 (-2.73)	-4.18 (-3.16)
DVU0310 (<i>fliH</i>)	Flagellum-specific ATP synthase FliH	-0.27 (-0.45)	-0.61 (-1.07)	-0.78 (-1.09)	-0.92 (-1.43)	-0.31 (-0.26)	-1.23 (-1.55)
DVU0311	Flagellar assembly protein FliH, putative	-0.53 (-0.78)	-0.58 (-0.99)	-0.54 (-0.57)	-0.86 (-0.92)	-0.94 (-1.01)	-0.66 (-0.51)
DVU0312 (<i>fliG</i>)	Flagellar motor switch protein FliG	-0.92 (-1.40)	-0.80 (-1.17)	-0.24 (-0.32)	-0.17 (-0.22)	-0.69 (-0.96)	-0.7 (-0.99)
DVU0313 (<i>fliF</i>)	Flagellar M-ring protein FliF	-1.35 (-1.38)	-1.83 (-1.86)	-0.75 (-0.68)	-1.05 (-0.96)	-0.69 (-1.19)	-0.91 (-1.64)
DVU0314 (<i>fliE</i>)	Flagellar basal body component FliE	-1.00 (-1.12)	-1.55 (-1.69)	-1.17 (-1.4)	-1.31 (-1.59)	-1.63 (-2.56)	-1.15 (-1.53)
DVU0315 (<i>flgC</i>)	Flagellar basal-body rod protein FlgC	-1.55 (-2.02)	-1.98 (-2.43)	-1.59 (-1.51)	-1.65 (-1.55)	-2.13 (-2.21)	-2.07 (-2.10)
DVU0316 (<i>flgB</i>)	Flagellar basal-body rod protein FlgB	-0.20 (-0.32)	0.02 (0.03)	0.25 (0.37)	0.26 (0.37)	-0.29 (-0.37)	-0.79 (-0.93)
DVU0512	Flagellar basal-body rod protein, putative	-0.24 (-0.30)	-0.61 (-0.76)	0.35 (0.48)	0.27 (0.37)	-2.08 (-2.01)	-1.85 (-1.78)
DVU0513 (<i>flgG</i>)	Flagellar basal-body rod protein FlgG	-0.25 (-0.33)	-1.32 (-2.05)	-1.61 (-1.20)	-1.71 (-1.26)	-1.66 (-0.93)	-1.94 (-1.16)
DVU0514	FlgA family protein	0.37 (0.48)	0.15 (0.19)	0.49 (0.51)	0.23 (0.23)	-1.26 (-1.01)	-0.88 (-0.63)
DVU0515 (<i>flgH</i>)	Flagellar L-ring protein FlgH	-0.56 (-1.00)	-0.73 (-1.3)	-0.78 (-1.19)	-0.57 (-0.86)	-1.46 (-2.32)	-1.58 (-2.49)
DVU0516 (<i>flgI</i>)	Flagellar P-ring protein FlgI	-0.46 (-0.68)	-0.22 (-0.36)	-0.68 (-1.08)	-0.94 (-1.37)	-1.76 (-2.05)	-2.15 (-1.85)
DVU0517	Peptidase, M23/M37 family	-1.87 (-2.13)	-2.43 (-2.68)	-1.35 (-1.75)	-2.10 (-2.73)	-1.27 (-0.83)	-2.32 (-2.19)
DVU0518	Hypothetical protein	-3.06 (-3.97)	-3.67 (-4.77)	-2.91 (-3.9)	-3.46 (-4.96)	-2.86 (-1.88)	-4.41 (-5.72)
DVU0519	Flagellar hook-associated protein FlgK, putative	-1.79 (-3.14)	-1.76 (-3.16)	-1.28 (-1.47)	-1.26 (-1.40)	-1.85 (-1.56)	-1.99 (-1.69)
DVU0520	Flagellar hook-associated protein FlgL, putative	-0.74 (-0.83)	-1.31 (-1.48)	-0.25 (-0.27)	-0.6 (-0.67)	-0.15 (-0.11)	-1.30 (-1.90)
DVU0521 (<i>csrA</i>)	Carbon storage regulator	-0.14 (-0.26)	-0.16 (-0.29)	-0.35 (-0.64)	-0.26 (-0.47)	0.45 (0.71)	-0.48 (-0.87)
DVU0522	Conserved hypothetical protein	-0.51 (-0.92)	-0.52 (-0.94)	-0.06 (-0.09)	-0.23 (-0.4)	0.21 (0.37)	-0.25 (-0.36)
DVU0523 (<i>flgM</i>)	Negative regulator of flagellin synthesis FlgM	-1.60 (-2.61)	-1.14 (-1.96)	-2.08 (-1.93)	-1.99 (-1.85)	-0.62(-0.48)	-1.69 (-1.43)
DVU0524	Hypothetical protein	-1.85 (-3.23)	-1.41 (-2.28)	-1.18 (-2.08)	-1.78 (-3.40)	-1.17 (-1.95)	-2.19 (-3.46)

Abbreviations: An, ancestor DvH; ATP, adenosine triphosphate; DVU, *Desulfovibrio vulgaris*; EC, strain isolated from population No.3 evolved under control condition; ES, strain isolated from population No.9 evolved under salt stress condition; LS4D-100, LS4D + 100 mM NaCl; LS4D-250, LS4D + 250 mM NaCl.

Log₂R ratios are shown with Z score in parentheses. Boldface indicates more than twofolds of expression changes.

regulator), DVU0942 (*fur*, ferric uptake regulator), DVU0629 (transcriptional regulator, TetR family), DVU0138 (response regulator), DVU3187 (*hup-4*, DNA-binding protein HU (heat unstable)), DVU1995 (*rsbV*, anti-anti-sigma factor) and DVU0408 encoding a response regulator/sensory box/GGDEF (Gly-Gly-Asp-Glu-Phe) domain/EAL (Glu-Ala-Leu) domain protein.

Transcriptional changes of genes involved in other gene categories such as 'lipid transport and metabolism' or 'replication, recombination and repair' are listed in Supplementary Table S1. These data were interpreted to indicate that ES9-11 adaptation to NaCl had occurred at the level of gene

expression, potentially leading to increased biosynthesis or transport of amino acids, cation effluxes and energy production but decreased motility.

Accumulation of organic solutes in evolved D. vulgaris
Metabolite measurements were carried out to determine whether the transcriptional changes were reflected at the metabolite level. The total abundances of 23 detected metabolites (Supplementary Table S2) were much higher in NaCl-evolved ES9-11 and control-evolved EC3-10 relative to the ancestral strain when grown in control medium (Figure 3a). However, under NaCl stress conditions, ES9-11

Table 3 Expression changes of genes involved in energy production and conversion or signal transduction and transcription in strain ES

DVU Nos.	Annotation	LS4D		LS4D-100		LS4D-250	
		ES vs An	ES vs EC	ES vs An	ES vs EC	ES vs An	ES vs EC
DVU3107	Cytochrome c family protein	1.17 (2.06)	2.08 (2.77)	1.20 (1.82)	2.21 (3.13)	1.47 (1.72)	2.35 (3.75)
DVU0624	NapC/NirT cytochrome c family protein	0.34 (0.64)	0.54 (1.05)	0.56 (1.09)	0.61 (1.16)	1.00 (1.97)	0.24 (0.47)
DVU0625	Cytochrome c nitrite reductase, catalytic subunit NfrA, putative	0.16 (0.27)	0.58 (0.93)	0.25 (0.38)	0.34 (0.56)	1.35 (1.97)	1.06 (1.63)
DVU0702	Cytochrome c family protein	0.16 (0.3)	0.43 (0.78)	−0.06 (−0.08)	0.21 (0.32)	1.24 (1.85)	0.02 (0.03)
DVU1817	Cytochrome c-553 (<i>cyf</i>)	0.52 (0.93)	0.69 (1.23)	0.68 (1.18)	0.88 (1.61)	1.31 (2.51)	0.48 (0.90)
DVU0253	Oxidoreductase, FAD/iron-sulfur cluster-binding domain protein	0.72 (1.28)	2.24 (3.75)	0.56 (0.92)	2.14 (3.8)	1.30 (2.22)	1.31 (1.96)
DVU2645	Na ⁺ /H ⁺ antiporter family protein	1.53 (1.96)	1.30 (1.29)	1.28 (1.16)	0.79 (0.63)	0.22 (0.16)	−0.29 (−0.20)
DVU2103	Iron-sulfur cluster-binding/ATPase domain protein	1.76 (1.40)	2.16 (2.93)	0.98 (1.68)	1.89 (3.12)	0.26 (0.19)	0.93 (0.91)
DVU2104	Iron-sulfur cluster-binding/ATPase domain protein	1.50 (0.92)	3.15 (2.44)	0.84 (0.58)	1.17 (0.60)	1.59 (1.61)	−0.46 (−0.33)
DVU0531	hmc operon protein 6	0.59 (0.76)	1.05 (1.21)	1.25 (2.00)	1.08 (1.25)	1.49 (1.40)	−0.17 (−0.22)
DVU0532	hmc operon protein 5	2.34 (1.94)	1.40 (1.56)	1.43 (1.13)	0.83 (0.73)	2.46 (2.33)	0.07 (0.09)
DVU0533	hmc operon protein 4	1.90 (1.25)	0.44 (0.50)	1.64 (2.01)	0.70 (0.85)	3.03 (2.16)	−0.44 (−0.50)
DVU0534	hmc operon protein 3	0.43 (0.52)	−0.32 (−0.45)	0.96 (1.38)	0.33 (0.47)	2.71 (1.57)	−0.1 (−0.12)
DVU0535	hmc operon protein 2	NA	NA(NA)	2.03 (3.77)	2.26 (3.11)	0.04 (0.05)	0.41 (0.31)
DVU0536	High-molecular-weight cytochrome C (<i>hmcA</i>)	0.98 (1.56)	1.75 (2.27)	1.28 (1.61)	1.51 (1.38)	1.15 (1.50)	−0.30 (−0.40)
DVU0305 (<i>fd II</i>)	Ferredoxin II	0.41 (0.64)	2.13 (3.46)	1.61 (2.42)	1.21 (1.96)	2.06 (3.64)	0.32 (0.58)
DVU0384	Flavodoxin (<i>flr</i>)	0.33 (0.61)	0.24 (0.43)	0.67 (1.28)	0.59 (1.14)	1.69 (2.33)	0.78 (1.47)
DVU2451	L-lactate permease family protein	0.85 (1.67)	0.94 (1.77)	1.31 (2.45)	1.26 (2.19)	1.72 (3.18)	0.22 (0.41)
DVU2683	L-lactate permease family protein	0.54 (0.94)	0.20 (0.34)	1.17 (1.86)	0.13 (0.18)	1.39 (1.32)	−0.11 (−0.2)
DVU1780	Conserved hypothetical protein	−1.74 (−2.88)	−1.86 (−2.09)	−1.75 (−3.31)	−1.39 (−2.66)	−0.85 (−0.72)	−1.55 (−1.47)
DVU1781	Conserved hypothetical protein	−3.91 (−6.41)	−3.4 (−5.38)	−4.00 (−7.15)	−2.89 (−5.22)	−3.93 (−3.98)	−4.17 (−3.98)
DVU1782	Iron-sulfur cluster-binding protein	−3.16 (−4.39)	−3.27 (−4.03)	−3.01 (−4.88)	−3.23 (−5.58)	−3.04 (−1.98)	−3.14 (−2.64)
DVU1783	Cysteine-rich domain protein	−2.76 (−4.53)	−2.84 (−4.42)	−1.72 (−2.20)	−1.53 (−2.00)	−2.89 (−4.25)	−1.97 (−2.64)
DVU2286	Hydrogenase, CooM subunit, putative	−0.75 (−1.38)	−1.04 (−1.86)	−1.14 (−1.98)	−1.50 (−2.58)	−0.83 (−1.25)	−0.73 (−1.06)
DVU2287	Hydrogenase, CooK subunit, selenocysteine-containing, putative	NA	NA	NA	NA	NA	NA
DVU2288	Hydrogenase, CooL subunit, putative	−0.90 (−1.5)	−1.65 (−2.72)	−1.27 (−2.06)	−1.85 (−2.91)	−0.97 (−1.58)	−0.58 (−0.90)
DVU2289	Hydrogenase, CooX subunit, putative	−0.48 (−0.85)	−1.22 (−2.18)	−0.98 (−1.68)	−1.29 (−2.13)	−0.70 (−1.17)	−0.56 (−0.88)
DVU2290	Hydrogenase, CooU subunit, putative	−1.08 (−2.07)	−1.41 (−2.67)	−1.32 (−2.31)	−1.36 (−2.31)	−0.98 (−1.55)	−0.69 (−1.06)
DVU2291	Carbon monoxide-induced hydrogenase CooH, putative	−0.60 (−1.13)	−0.97 (−1.82)	−0.79 (−1.41)	−1.12 (−2.04)	−0.71 (−1.24)	−0.63 (−1.04)
DVU2292	Hydrogenase nickel insertion protein HypA (<i>hypA</i>)	−1.02 (−1.74)	−1.43 (−2.27)	−1.05 (−1.93)	−1.16 (−2.11)	−0.83 (−1.44)	−0.25 (−0.41)
DVU2293	Iron-sulfur protein CooF (<i>cooF</i>)	−0.75 (−1.42)	−0.68 (−1.28)	−0.67 (−1.27)	−0.74 (−1.40)	−0.53 (−0.95)	−0.24 (−0.43)
<i>Signal transduction and transcription</i>							
DVU0598	Carbon-starvation protein A, putative	3.56 (6.62)	1.04 (2.03)	4.49 (7.27)	1.14 (1.53)	7.20 (4.18)	0.49 (0.82)
DVU0599	Carbon-starvation protein A, putative	4.02 (7.36)	0.03 (0.05)	4.56 (8.15)	0.08 (0.16)	5.14 (6.35)	0.40 (0.77)
DVU0529	Transcriptional regulator, rrf2 protein, putative	1.35 (1.68)	2.10 (2.02)	1.73 (2.54)	1.89 (2.09)	2.28 (2.46)	0.50 (0.53)
DVU0530	Response regulator, rrf1 protein	0.81 (1.12)	0.95 (1.16)	1.73 (2.34)	0.81 (1.25)	1.99 (1.90)	0.09 (0.14)
DVU2114 (<i>atoC</i>)	Sigma-54-dependent transcriptional regulator/response regulator	0.88 (1.53)	1.31 (2.45)	0.93 (1.38)	1.22 (2.07)	1.89 (2.37)	1.21 (1.77)
DVU0942 (<i>fur</i>)	Ferric uptake regulator	0.49 (1.26)	1.40 (2.05)	0.78 (0.86)	1.05 (1.67)	1.88 (1.22)	0.43 (0.75)
DVU0629	Transcriptional regulator, TetR family	0.60 (1.12)	1.46 (2.45)	0.74 (1.21)	1.30 (2.44)	1.55 (2.10)	0.55 (0.98)
DVU0630	Hypothetical protein	0.88 (1.62)	1.13 (2.02)	1.19 (2.22)	1.21 (2.24)	1.86 (1.17)	1.00 (1.32)
DVU0138	Response regulator	0.58 (1.03)	1.29 (2.28)	0.41 (0.73)	1.12 (2.04)	1.54 (3.07)	0.86 (1.56)
DVU1516	Hypothetical protein	1.60 (1.16)	1.31 (1.07)	1.90 (1.74)	1.64 (1.5)	−0.15 (−0.13)	0.30 (0.25)
DVU1517	Transcriptional regulator cII, putative	1.75 (1.56)	1.79 (1.79)	1.63 (1.20)	1.76 (1.54)	0.71 (0.56)	−0.54 (−0.4)
DVU0006	Universal stress protein family	0.75 (1.47)	1.39 (2.66)	0.58 (0.97)	1.22 (2.09)	1.40 (2.55)	0.74 (1.39)
DVU3187 (<i>hup-4</i>)	DNA-binding protein HU	0.12 (0.24)	1.07 (1.95)	0.13 (0.20)	0.79 (1.30)	1.84 (3.15)	0.93 (1.79)
DVU2686	Peptidase, S24 family	0.66 (1.20)	1.60 (2.51)	0.61 (0.94)	0.91 (1.52)	1.60 (2.39)	0.44 (0.73)
DVU1995 (<i>rsbV</i>)	Anti-anti-sigma factor	0.74 (1.31)	1.14 (1.57)	0.02 (0.03)	0.28 (0.51)	1.62 (1.11)	2.29 (2.10)
DVU1967	Transcriptional regulator, rrf2 protein, putative	1.66 (2.15)	0.84 (1.01)	0.43 (0.35)	1.04 (1.15)	0.49 (0.49)	−0.11 (−0.10)
DVU1968	Oxidoreductase, putative	0.11 (0.13)	1.44 (2.05)	1.18 (1.04)	1.41 (1.23)	−0.40 (−0.34)	−0.96 (−0.90)
DVU1969	Hypothetical protein	1.81 (2.03)	0.73 (0.64)	1.44 (1.49)	1.93 (2.16)	−0.85 (−1.03)	−1.27 (−1.07)
DVU1970	Response regulator	1.16 (0.89)	1.08 (1.25)	1.74 (1.17)	1.42 (1.22)	0.09 (0.08)	−0.14 (−0.16)
DVU0408	Response regulator/sensory box/CGDEF domain/EAL domain protein	0.34 (0.66)	0.40 (0.76)	0.19 (0.35)	0.08 (0.14)	2.39 (1.53)	1.54 (1.44)
DVU0720	HAMP domain protein	0.05 (0.09)	0.51 (0.96)	0.12 (0.18)	0.24 (0.43)	2.39 (2.14)	0.94 (1.20)
DVU0606	Transcriptional regulator, ArsR family/methyltransferase, UbiE/COQ5 family	0.47 (0.91)	−0.19 (−0.37)	0.76 (1.18)	0.39 (0.69)	1.64 (2.90)	−0.18 (−0.32)
DVU1285	Response regulator	0.58 (1.08)	0.97 (1.55)	0.60 (0.95)	0.87 (1.65)	1.68 (1.23)	0.27 (0.41)
DVU1690	Transcriptional regulator, TetR family	−0.04 (−0.05)	0.81 (1.34)	−0.10 (−0.19)	0.01 (0.01)	1.74 (3.06)	0.58 (1.08)

Abbreviations: An, ancestor DvH; ATP, adenosine triphosphate; DVU, *Desulfovibrio vulgaris*; EC, strain isolated from population No.3 evolved under control condition; ES, strain isolated from population No.9 evolved under salt-stress condition; FAD, flavin adenine dinucleotide; HAMP, Histidine kinases, Adenyl cyclases, Methyl-accepting proteins and Phosphatase; HU, heat unstable; LS4D-100, LS4D + 100 mM NaCl; LS4D-250, LS4D + 250 mM NaCl; NA, not applicable.
Log₂R ratios are shown with Z score in parentheses. Boldface indicates more than twofolds of expression changes.

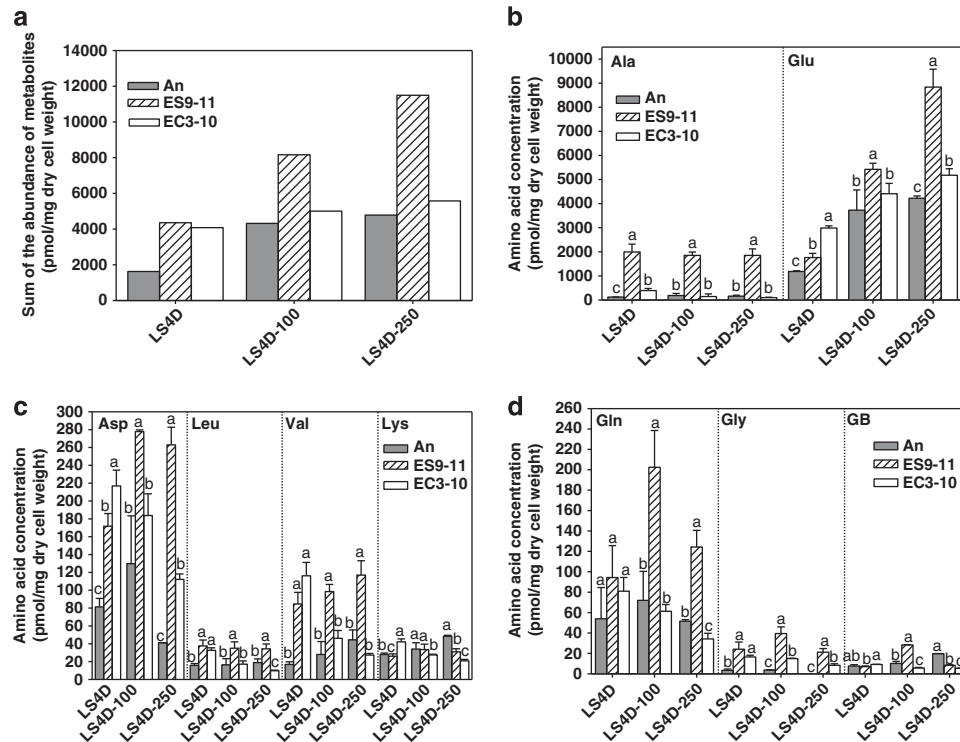


Figure 3 Accumulation of organic solutes in evolved *D. vulgaris* strains. The sums of detected organic solutes are much higher in NaCl-evolved ES9-11 in all culture conditions (a). Abundance changes of two abundant amino acids Glu and Ala are shown in (b). Changes of less abundant organic solutes such as Asp, Leu, Val and Lys (c), and induction of Gln, Gly and GB under low NaCl stress (d) are shown. Error bars indicate s.d. The significance of abundance changes is shown at the $P < 0.05$ level (*t*-test). LS4D-100, LS4D + 100 mM NaCl; LS4D-250, LS4D + 250 mM NaCl.

showed the capacity to greatly increase intracellular metabolites relative to An, in contrast to EC3-10 (Figure 3a). Glu and Ala were the two most abundant amino acids in ES9-11 and An under all the tested culture conditions (Supplementary Table S2). Significant abundance increases of Glu induced by NaCl stress was observed in ES9-11, but no significant abundance changes of Ala were induced by NaCl stress in ES9-11 and decreased Ala abundance under NaCl stress conditions were seen in EC3-10 (Figure 3b). Under no-NaCl stress, significant ($P < 0.05$) abundance increases of 12 metabolites, including Glu, Ala, Asp, Val, Met, Thr, Ile, Leu, Gly, Pyruvic acid, Phe and agmatine, and significant abundance decrease of Lys were detected in ES9-11 (Supplementary Table S2). Glu is likely the most important contributor to osmoprotection under NaCl stress. Other less abundant metabolites such as Asp and Val could contribute little osmoprotection (Figure 3c). Interestingly, abundances of Gln, Gly and GB in ES9-11 increased under 100-mM NaCl stress only. The abundance changes of metabolites such as Glu and Lys corresponded well with the transcriptional changes (Table 1). The metabolite data suggested important roles of Glu, possibly Ala, Asp and Val in relieving NaCl stress, while other organic solutes such as Gln, Gly and GB might contribute under low NaCl stress only.

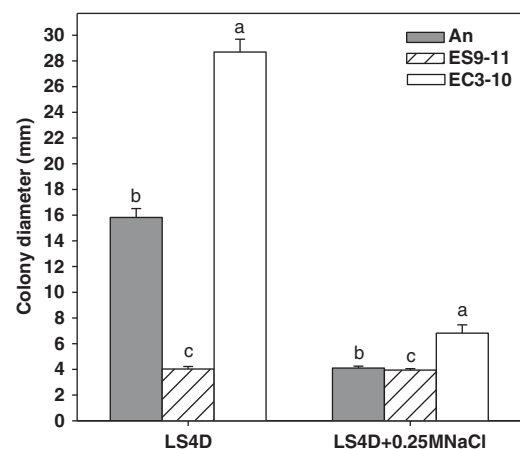


Figure 4 Changes of cell motility in evolved *D. vulgaris* strains under no-NaCl stress or 250-mM NaCl stress conditions. A *t*-test was performed to assess the significance of difference among strains ($P < 0.0001$).

Decreased cell motility in evolved *D. vulgaris*

To test whether decreased expression of genes involved in flagellar assembly impacted cell motility, cell motility was evaluated by measuring the colony diameter after 4 days of incubation on soft agar. Decreases of cell motility induced by 250-mM NaCl stress were observed for NaCl-evolved ES9-11 ($P = 0.0216$), control-evolved EC3-10

($P < 0.0001$) and An ($P < 0.0001$), and motility of ES9-11 was the lowest under no-stress and NaCl-stress conditions ($P < 0.0001$) (Figure 4), consistent with decreased expressions of flagellar system genes in ES9-11 in all the culture conditions. The fastest growth but lowest motility in ES9-11 under no-NaCl stress and 250-mM NaCl stress suggests the possibility of more energy flow towards osmoprotection with less energy available for other functions, such as motility.

Changes of PLFA composition in evolved *D. vulgaris*
PLFA profiling was investigated to test whether the expression changes of genes involved in lipid metabolism was reflected in the cell membrane PLFA composition. Under no-NaCl stress, there was a significant increase of the UI of PLFAs in NaCl-evolved ES9-11 and control-evolved EC3-10 compared with An. Under 250-mM NaCl stress, unlike the significant ($P = 0.004$) decrease of UI in An, no significant changes of UI were found in ES9-11 or EC3-10 (Figure 5). PLFA composition changes under no-NaCl stress or 250-mM NaCl stress conditions were shown in Figure 6. Under no-NaCl stress, increases of unsaturated 16:1 ω 7c and saturated 16:0 were found in ES9-11 and EC3-10, but significant higher percentages of fatty acids 16:1 ω 7c ($P = 0.0414$) and 16:0 ($P = 0.0011$) were found in ES9-11 than EC3-10; increase of unsaturated i16:1 H was only detected in ES9-11; decreases of fatty acids i15:0, i16:0, i17:1 ω 9c, i17:0 and 18:0 were detected in ES9-11 and EC3-10, but percentages of i15:0 ($P = 0.0123$) and i16:0 ($P = 0.001$) were significantly different between ES9-11 and EC3-10 (Figure 6a). Under 250-mM NaCl stress, different PLFA composition changes were found in ES9-11, EC3-10 or An (Figure 6b). In addition to the increase of 18:1 ω 7c and decrease of 17:0 seen in all the strains, unique

changes in ES9-11 included increased i17:1 ω 9c, a17:1 ω 9c, i15:0 and decreased 16:1 ω 7c and 16:0. In conclusion, unsaturated i16:1 H and 16:1 ω 7c might be the major fatty acids contributing to the increase of UI under no-NaCl stress. Branched PLFAs, including i17:1 ω 9c, a17:1 ω 9c and i15:0, might have important roles in keeping proper membrane fluidity under NaCl stress.

Discussion

Experimental evolution with microbes has been employed to address evolution-related theories and study genetically simple traits (Elena and Lenski, 2003; Kawecki *et al.*, 2012). NaCl tolerance is a complex trait involving several pathways (Warringer *et al.*, 2003; Dhar *et al.*, 2011). This study provides an example of selection of NaCl tolerance trait through experimental evolution. Three main physiological components of NaCl stress response, including adaptation time to NaCl stress, growth rate and efficiency of growth in NaCl stress (Warringer *et al.*, 2003), have been improved in

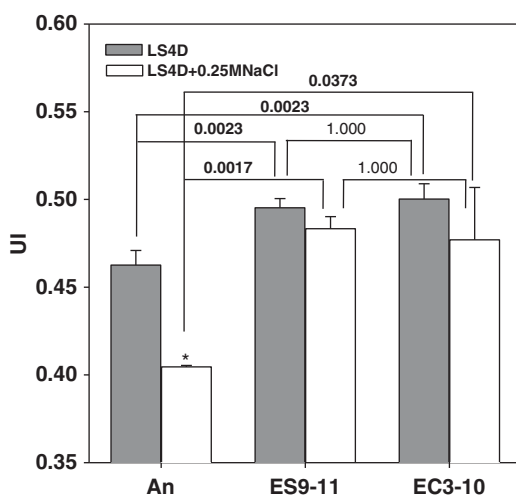


Figure 5 Changes of UI of PLFA in evolved *D. vulgaris* strains under no-NaCl stress or 250-mM NaCl stress conditions. Bold font indicates $P < 0.05$. Error bars indicate s.d. * $P < 0.05$.

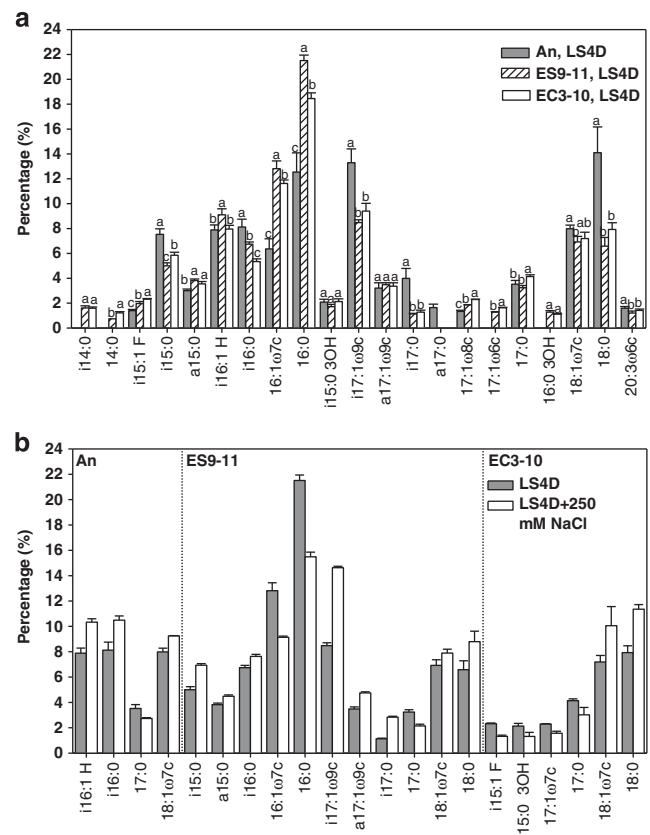


Figure 6 PLFA composition changes in evolved *D. vulgaris* strains. Under no-NaCl stress, there are many PLFA composition changes in NaCl-evolved ES9-11 and control-evolved EC3-10 compared with ancestral strain An (a). The significance of abundance changes is shown at the $P < 0.05$ level (*t*-test). Under 250-mM NaCl stress, composition changes ($P < 0.05$) of PLFAs are different in strains ES9-11, EC3-10 or An (b).

evolved *D. vulgaris*. Mechanisms underlying the phenotypic adaptation include significant changes in favor of NaCl tolerance in gene expression, metabolites abundance and PLFA profile.

Data from this study suggest that accumulation of organic solutes is important for NaCl adaptation during evolution. Upon exposure to NaCl stress, physiological changes are triggered by the rapid efflux of cellular water. Immediate responses such as accumulation of intracellular K^+ and Glu were found in *E. coli* (McLaggan *et al.*, 1994); long-term osmoadaptive responses are accumulation of non-ionic compatible solutes, which interfere little with most cytoplasmic enzymes (Sleator and Hill, 2002). Glu appears to be the most important osmoprotectant in evolved *D. vulgaris*. Glu was the most abundant organic solute in ES9-11 and its abundance significantly increased under NaCl stress. By contrast, no significant abundance changes of Ala were induced by NaCl stress. Glu is a commonly accumulated microbial osmolyte (Botsford and Lewis, 1990; Botsford *et al.*, 1994; McLaggan *et al.*, 1994); however, an osmoregulatory role for Ala during NaCl stress has rarely been reported (Thomas and Shanmugasundaram, 1991). Accumulation of Ala was observed in *D. vulgaris* exposed to 250-mM NaCl stress for about 100 h (He *et al.*, 2010), but further study is required to confirm the role of Ala in osmoprotection during evolution. Addition of Lys in medium did not improve growth of *D. vulgaris* under NaCl stress (He *et al.*, 2010), significantly decreased abundance of Lys was observed in NaCl-evolved ES9-11, confirming that Lys is not an osmoprotectant in NaCl stress response of *D. vulgaris*. GB production was lower in NaCl-evolved ES9-11 than the ancestral strain under 250-mM NaCl stress, which was opposite to its increased abundance in *D. vulgaris* exposed to 250 mM NaCl for 4 h (Mukhopadhyay *et al.*, 2006). However, abundance of Gln, Gly and GB increased under 100-mM NaCl stress. Accumulation of different sets of organic solutes under low or high NaCl stresses has been found in the facultative anaerobe *Erwinia chrysanthemi* (Goude *et al.*, 2004). It is likely that different sets of organic solutes were used as osmoprotectants to cope with low or high NaCl stresses in *D. vulgaris*. Further studies are required to identify other non-ionic compatible solutes important for osmoadaptation of *D. vulgaris* to NaCl stress.

PLFA composition changes is another important aspect of NaCl adaptation in *D. vulgaris*. It is well known that NaCl stress increases membrane rigidity and causes membrane PLFA composition changes in bacteria (Kates, 1986; Los and Murata, 2004). Possible role of unsaturated branched PLFA i17:1 ω 9c in *D. vulgaris* exposed to 250-mM NaCl stress was reported (Mukhopadhyay *et al.*, 2006). In NaCl-evolved ES9-11, under no-NaCl stress, unsaturated PLFAs such as 16:1 ω 9c and i16:1 H appeared to be the major contributors for increased UI; under 250-mM NaCl stress, in addition to i17:1 ω 9c, percentages

of branched PLFAs such as a17:1 ω 9c and i15:0 significantly increased, confirming the roles of branched PLFAs in maintaining proper membrane fluidity adaptation of *D. vulgaris* to NaCl stress.

Other physiological aspects important for adaptation to NaCl stress were suggested by gene expression changes in NaCl-evolved ES9-11, such as: increased energy conversion and detoxification of Na^+ possibly resulted from increased expressions of two lactate permease family protein genes and Na^+/H^+ antiporter gene, respectively; and role of *fur* in gene regulation. These gene expression changes were not seen in NaCl stress responses in literature. Possible role of *fur* in osmotic stress of *D. vulgaris* was suggested in previous deletion mutant study (Bender *et al.*, 2007) and *Fur* was found essential for growth of *Helicobacter pylori* in NaCl-challenged cells (Gancz and Merrell, 2011). Further study is needed to identify the role of *fur* in NaCl adaptation of *D. vulgaris*. Some gene expression changes were consistent with previous results, namely NaCl shock response and short-term adaptation to NaCl stress in *D. vulgaris* or other bacteria. For example, the repression of flagella assembly genes (Steil *et al.*, 2003; Liu *et al.*, 2005; Mukhopadhyay *et al.*, 2006), increased expression of iron-uptake genes (Hoffmann *et al.*, 2002; Steil *et al.*, 2003; He *et al.*, 2010), cation efflux genes (Mukhopadhyay *et al.*, 2006) and *hmc* operon genes (Dolla *et al.*, 2000). Lacking of increased expression levels of genes related to general stress responses, such as heat-shock genes (He *et al.*, 2010; Cameron *et al.*, 2012) important for stress-induced protein folding and other damages, suggests the adaptation to NaCl stress in NaCl-evolved ES9-11.

Certain level of NaCl tolerance improvement was observed in control-evolved EC3-10. The $[Na^+]$ in LS4D is about 210 mM, which is higher compared with the medium used by ATCC (about 90 mM). Higher $[Na^+]$ in LS4D may be responsible for enhancing NaCl tolerance in EC3-10. Therefore, ionic strength of the culture medium is an important factor to be considered in experiment design, especially in experimental evolution.

A conceptual model of NaCl adaptation was proposed based on the data with single-colony isolates from *D. vulgaris* evolved under low NaCl stress (Figure 7). Constant exposure to low NaCl stress induced dramatic transcriptional changes of functional genes and regulatory genes. Altered gene expressions (basal changes) when cultured in medium without NaCl amendment suggests the possibility of genetic adaptation. The basal increase of Na^+/H^+ antiporter expression and the increased expression of a cation efflux protein encoding gene in response to NaCl stress might enable efficient ionic detoxification. Basal increases and increased expression of amino-acid synthesis and transport genes lead to intracellular accumulation of compatible solutes. Also, increased expression of lactate-uptake genes and genes involved in energy

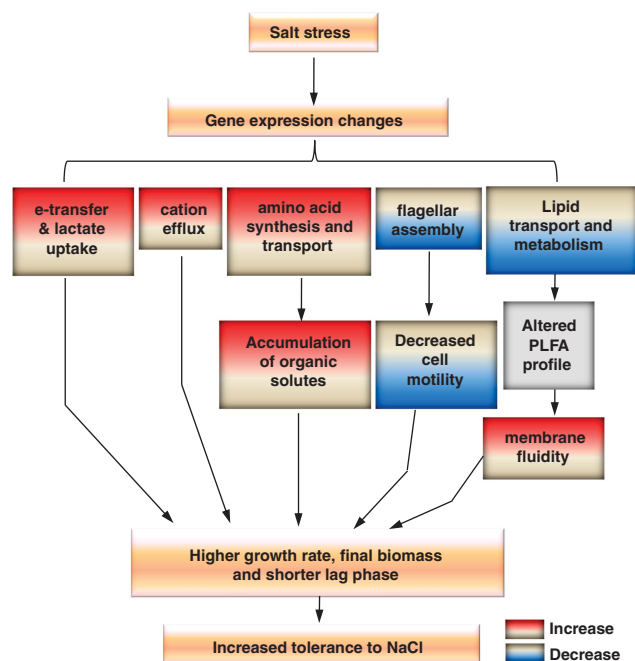


Figure 7 A conceptual model of adaptation to NaCl stress in evolved *D. vulgaris*. Gene expression changes induced by NaCl stress, accumulation of organic solutes, increased membrane fluidity, decreased cell motility, potentially increased exclusion of Na^+ and increased energy metabolism contribute to increased tolerance to NaCl in evolved *D. vulgaris*.

conversion ensure that sufficient energy is produced for cellular activities. In addition, decreased expression of flagellar assembly genes resulting in decreased cell motility allows more energy available for osmoprotection. Changes of genes involved in lipid metabolism may contribute to the significant changes of PLFA composition. The basal increase of unsaturated or unsaturated branched PLFA under no-NaCl stress and the unique increase of unsaturated or unsaturated branched PLFA under NaCl stress increases the membrane fluidity, which is critical for proper cellular function. Expression changes of regulatory genes under no-stress and NaCl-stress conditions ensure the rapid adjustment of gene expression to meet the challenges of NaCl stress. As a result, the inhibitory effect of NaCl stress on growth of *D. vulgaris* is conquered to a great extent: an increased growth rate and final biomass but shortened lag phase were observed for the NaCl-evolved strain ES9-11 under NaCl stress.

Conflict of Interest

The authors declare no conflict of interest.

Acknowledgements

This work conducted by ENIGMA—Ecosystems and Networks Integrated with Genes and Molecular

Assemblies (<http://enigma.lbl.gov>)—a Scientific Focus Area Program at Lawrence Berkeley National Laboratory, was supported by the Office of Science, Office of Biological and Environmental Research, US Department of Energy under Contract No. DE-AC02-05CH11231.

References

- Baidoo EEK, Benke PI, Neuss C, Pelzing M, Kruppa G, Leary JA *et al.* (2008). Capillary electrophoresis-fourier transform ion cyclotron resonance mass spectrometry for the identification of cationic metabolites via a pH-mediated stacking-transient isotachophoretic method. *Anal Chem* **80**: 3112–3122.
- Bender KS, Yen H-CB, Hemme CL, Yang Z, He Z, He Q *et al.* (2007). Analysis of a ferric uptake regulator (Fur) mutant of *Desulfovibrio vulgaris* Hildenborough. *Appl Environ Microbiol* **73**: 5389–5400.
- Botsford JL, Alvarez M, Hernandez R, Nichols R. (1994). Accumulation of glutamate by *Salmonella typhimurium* in response to osmotic stress. *Appl Environ Microbiol* **60**: 2568–2574.
- Botsford JL, Lewis TA. (1990). Osmoregulation in *Rhizobium meliloti*: production of glutamic acid in response to osmotic stress. *Appl Environ Microbiol* **56**: 488–494.
- Cameron A, Frirdich E, Huynh S, Parker CT, Gaynor EC. (2012). Hyperosmotic stress response of *Campylobacter jejuni*. *J Bacteriol* **194**: 6116–6130.
- Chang YJ, Peacock AD, Long PE, Stephen JR, McKinley JP, Macnaughton SJ *et al.* (2001). Diversity and characterization of sulfate-reducing bacteria in groundwater at a uranium mill tailings site. *Appl Environ Microbiol* **67**: 3149–3160.
- Chhabra SR, He Q, Huang KH, Gaucher SP, Alm EJ, He Z *et al.* (2006). Global analysis of heat shock response in *Desulfovibrio vulgaris* Hildenborough. *J Bacteriol* **188**: 1817–1828.
- Dhar R, SÁGesser R, Weikert C, Yuan J, Wagner A. (2011). Adaptation of *Saccharomyces cerevisiae* to saline stress through laboratory evolution. *J Evol Biol* **24**: 1135–1153.
- Dolla A, Pohorelic BKJ, Voordouw JK, Voordouw G. (2000). Deletion of the *hmc* operon of *Desulfovibrio vulgaris* subsp. *vulgaris* Hildenborough hampers hydrogen metabolism and low-redox-potential niche establishment. *Arch Microbiol* **174**: 143–151.
- Elena SF, Lenski RE. (2003). Evolution experiments with microorganisms: the dynamics and genetic bases of adaptation. *Nat Rev Genet* **4**: 457–469.
- Elias DA, Suflita JM, McInerney MJ, Krumholz LR. (2004). Periplasmic cytochrome c3 of *Desulfovibrio vulgaris* is directly involved in H_2 -mediated metal but not sulfate reduction. *Appl Environ Microbiol* **70**: 413–420.
- Gancz H, Merrell DS. (2011). The *Helicobacter pylori* ferric uptake regulator (Fur) is essential for growth under sodium chloride stress. *J Microbiol* **49**: 294–298.
- Goude R, Renaud S, Bonnassie S, Bernard T, Blanco C. (2004). Glutamine, glutamate, and α -glucosylglycerate are the major osmotic solutes accumulated by *Erwinia chrysanthemi* strain 3937. *Appl Environ Microbiol* **70**: 6535–6541.

- He Q, Huang KH, He Z, Alm EJ, Fields MW, Hazen TC *et al.* (2006). Energetic consequences of nitrite stress in *Desulfovibrio vulgaris* Hildenborough, inferred from global transcriptional analysis. *Appl Environ Microbiol* **72**: 4370–4381.
- He Z, Zhou A, Baidoo E, He Q, Joachimiak MP, Benke P *et al.* (2010). Global transcriptional, physiological, and metabolite analyses of the responses of *Desulfovibrio vulgaris* Hildenborough to salt adaptation. *Appl Environ Microbiol* **76**: 1574–1586.
- Hoffmann T, Schutz A, Brosius M, Volker A, Volker U, Bremer E. (2002). High-salinity-induced iron limitation in *Bacillus subtilis*. *J Bacteriol* **184**: 718–727.
- Jebbar M, Talibart R, Gloux K, Bernard T, Blanco C. (1992). Osmoprotection of *Escherichia coli* by ectoine: uptake and accumulation characteristics. *J Bacteriol* **174**: 5027–5035.
- Kates M. (1986). Influence of salt concentration on the membrane lipids of halophilic bacteria. *FEMS Microbiol Rev* **39**: 95–101.
- Kawecki TJ, Lenski RE, Ebert D, Hollis B, Olivieri I, Whitlock MC. (2012). Experimental evolution. *Trends Ecol Evol* **27**: 547–560.
- Ko R, Smith LT, Smith GM. (1994). Glycine betaine confers enhanced osmotolerance and cryotolerance on *Listeria monocytogenes*. *J Bacteriol* **176**: 426–431.
- Liu Y, Gao W, Wang Y, Wu L, Liu X, Yan T *et al.* (2005). Transcriptome analysis of *Shewanella oneidensis* MR-1 in response to elevated salt conditions. *J Bacteriol* **187**: 2501–2507.
- Los DA, Murata N. (2004). Membrane fluidity and its roles in the perception of environmental signals. *Biochim Biophys Acta* **1666**: 142–157.
- Lovley DR, Phillips EJP. (1994). Reduction of chromate by *Desulfovibrio vulgaris* and its c3 cytochrome. *Appl Environ Microbiol* **60**: 726–728.
- Lovley DR, Widman PK, Woodward JC, Phillips EJ. (1993). Reduction of uranium by cytochrome c3 of *Desulfovibrio vulgaris*. *Appl Environ Microbiol* **59**: 3572–3576.
- López CS, Heras H, Garda H, Ruzal S, Sánchez-Rivas C, Rivas E. (2000). Biochemical and biophysical studies of *Bacillus subtilis* envelopes under hyperosmotic stress. *Int J Food Microbiol* **55**: 137–142.
- McLaggan D, Naprstek J, Buurman ET, Epstein W. (1994). Interdependence of K⁺ and glutamate accumulation during osmotic adaptation of *Escherichia coli*. *J Biol Chem* **269**: 1911–1917.
- Mukhopadhyay A, He Z, Alm EJ, Arkin AP, Baidoo EE, Borglin SC *et al.* (2006). Salt stress in *Desulfovibrio vulgaris* Hildenborough: an integrated genomics approach. *J Bacteriol* **188**: 4068–4078.
- Muyzer G, Stams AJM. (2008). The ecology and biotechnology of sulphate-reducing bacteria. *Nat Rev Micro* **6**: 441–454.
- Postgate JR. (1984). *The Sulfate-Reducing Bacteria*. Cambridge University Press: Cambridge, UK.
- Roberts M. (2005). Organic compatible solutes of halotolerant and halophilic microorganisms. *Saline Syst* **1**: 5.
- Ruess L, Schütz K, Migge-Kleian S, Häggblom MM, Kandeler E, Scheu S. (2007). Lipid composition of collembola and their food resources in deciduous forest stands—implications for feeding strategies. *Soil Biol Biochem* **39**: 1990–2000.
- Russell N. (1989). Adaptive modifications in membranes of halotolerant and halophilic microorganisms. *J Bioenerg Biomembr* **21**: 93–113.
- Sleator RD, Hill C. (2002). Bacterial osmoadaptation: the role of osmolytes in bacterial stress and virulence. *FEMS Microbiol Rev* **26**: 49–71.
- Steil L, Hoffmann T, Budde I, Volker U, Bremer E. (2003). Genome-wide transcriptional profiling analysis of adaptation of *Bacillus subtilis* to high salinity. *J Bacteriol* **185**: 6358–6370.
- Strøm AR, Kaasen I. (1993). Trehalose metabolism in *Escherichia coli*: stress protection and stress regulation of gene expression. *Mol Microbiol* **8**: 205–210.
- Thomas SP, Shanmugasundaram S. (1991). Osmoregulatory role of alanine during salt stress in the nitrogen fixing cyanobacterium *Anabaena* sp. 287. *Biochem Int* **23**: 93–102.
- Warringer J, Ericson E, Fernandez L, Nerman O, Blomberg A. (2003). High-resolution yeast phenomics resolves different physiological features in the saline response. *Proc Natl Acad Sci USA* **100**: 15724–15729.
- Welsh DT, Lindsay YE, Caumette P, Herbert RA, Hannan J. (1996). Identification of trehalose and glycine betaine as compatible solutes in the moderately halophilic sulfate reducing bacterium, *Desulfovibrio halophilus*. *FEMS Microbiol Lett* **140**: 203–207.
- Whatmore AM, Chudek JA, Reed RH. (1990). The effects of osmotic upshock on the intracellular solute pools of *Bacillus subtilis*. *J Gen Microbiol* **136**: 2527–2535.
- Zhou A, He Z, Redding-Johanson AM, Mukhopadhyay A, Hemme CL, Joachimiak MP *et al.* (2010). Hydrogen peroxide-induced oxidative stress responses in *Desulfovibrio vulgaris* Hildenborough. *Environ Microbiol* **12**: 2645–2657.
- Zhou J, Bruns MA, Tiedje JM. (1996). DNA recovery from soils of diverse composition. *Appl Environ Microbiol* **62**: 316–322.
- Zhou J, He Q, Hemme CL, Mukhopadhyay A, Hillesland K, Zhou A *et al.* (2011). How sulfate reducing microorganisms cope with stress: lessons from systems biology. *Nat Rev Microbiol* **9**: 452–466.

Supplementary Information accompanies this paper on The ISME Journal website (<http://www.nature.com/ismej>)